

9

Hybrid Variational Principles of Elastostatics I

TABLE OF CONTENTS

Page

TABLE OF CONTENTS

Page

§9.1. Nomenclature

In Chapter 6 the variational principles of linear elasticity were classified as single-field and multi-field. For the latter we expand now the classification as follows:

$$\text{Variational principles} \begin{cases} \text{Single-field} \\ \text{Multifield} \end{cases} \begin{cases} \text{Mixed (a.k.a. "pure mixed")} \\ \text{Hybrid} \end{cases} \begin{cases} \text{Internally single field} \\ \text{Internally multifield} \end{cases} \quad (9.1)$$

Single-field and mixed principles have been covered in previous chapters. In this Chapter we begin the study of hybrid functionals with FEM applications in mind.

Hybrid functionals have one or more master fields that are defined only on interfaces. These principles represent an important extension to the classical principles of mechanics. As discussed below, these extensions were largely motivated by trying to improve and extend the power of finite elements models.

Finite elements based on hybrid functionals, called *hybrid elements*, were constructed in the early 1960s. The original elements were quite limited in their ability to treat nonlinear and dynamic problems, as well as treatment of complicated geometries. However, such limitations are gradually disappearing as the fundamental concepts are better understood. Presently hybrid principles represent an important area of research in the construction of high performance finite elements, especially for plates and shells.

§9.2. Motivation

Why hybrid functionals? The general objective is to *relax* continuity conditions of fields. This idea has taken root in a surprisingly large number of technical applications, not all of which involve finite elements.

§9.2.1. Early Work

The original development came almost simultaneously from two widely different contexts:

Solid Mechanics. Prager proposed¹ the variational treatment of discontinuity conditions in elastic bodies by adding an interface potential. This extension was intended to handle physical discontinuities such as cracks, dislocations or material interfaces, at which internal field components, notably stresses, may jump.

Finite Elements. Pian² constructed continuum finite elements with stress assumptions but with displacement degrees of freedom. These are now known as *stress hybrids*, representing a tiny subclass of a vast population. Originally hybrids were constructed following a virtual-work recipe. A variational framework was not developed until the late sixties by Pian and Tong.³

¹ W. Prager, Variational principles for linear elastostatics for discontinuous displacements, strains and stresses, in *Recent Progress in Applied Mechanics*, The Folke-Odgvist Volume, ed. by B. Broger, J. Hult and F. Niordson, Almqvist and Wiksell, Stockholm, 463–474, 1967

² T. H. H. Pian, Derivation of element stiffness matrices by assumed stress distributions, *AIAA J.*, **2**, 1964, pp. 1333–1336.

³ T. H. H. Pian and P. Tong, Basis of finite element methods for solid continua, *Int. J. Numer. Meth. Engrg.*, **1**, 1969, pp.

§9.2.2. Recent Developments

For the next two decades (1970-1990) hybrid variational forms made slow progress in finite element applications. The mathematical basis is not easily accessible to students.⁴ The topic is plagued with “variational glitches” that have often led FEM researchers astray. There have been questions on the applicability to nonlinear and dynamic analysis.

The topic has revived over the past decade because of increasing interest in *model decomposition methods* for a myriad of applications: massively parallel computation, system identification, damage detection, optimization, coupling of nonmatched meshes, and multiscale analysis. All of these applications have in common the breakdown of a FEM model into pieces (substructures or subdomains) separated by interfaces. Hybrid functionals provide a general and elegant way of “gluing” those interfaces together.

§9.2.3. Improving FEM Models

The original motivation of hybrids for FEM was to alleviate the following difficulties noted in displacement-assumed elements.

Relaxed continuity requirements. Meeting the variationally-dictated continuity requirements in the construction of fully conforming displacement shape functions of some structural models, notably plate and shell elements, is difficult.⁵ Furthermore, continuity across elements of different type (for example, a beam element linked to a solid or shell element) is not easy to achieve.

Better displacement solution. Even after conforming plate and shell elements were developed, it was noted that performance for coarse meshes or irregular meshes was disappointing. The elements were generally over stiff, requiring computationally expensive fine meshes to deliver engineering accuracy.

Better stress solution. Not only the conforming elements tended to be over stiff in displacements, but stresses derived from them were often of poor accuracy and — worse of all from an engineering standpoint — unconservative in the sense that they underestimated the analytical values.

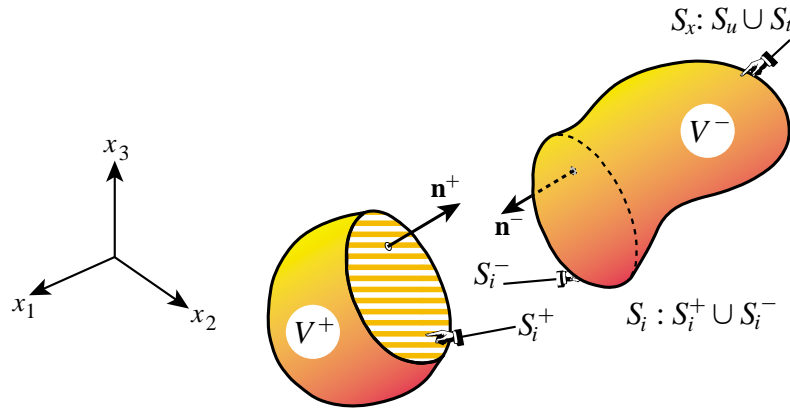
These three goals were accomplished for linear static analysis using hybrid elements. The extension to dynamic and nonlinear analysis was hampered initially by the lack of knowledge of interior displacements, which are needed to get mass and geometric stiffness matrices, respectively. This is gradually being solved with more powerful techniques.

At this point one may ask: why not use *mixed* variational principles instead of hybrids? Mixed principles are simpler to understand, and appear to address the goal of balanced accuracy directly.

3–29. See also T. H. H. Pian, Finite element methods by variational principles with relaxed continuity requirements, in *Variational Methods in Engineering*, Vol. 1, ed. by C. A. Brebbia and H. Tottenham, Southampton University Press, Southampton, U.K., 1973 A systematic classification of hybrid elements was undertaken by S. N. Atluri, On “hybrid” finite-element models in solid mechanics, In: *Advances in Computer Methods for Partial Differential Equations*. Ed. by R. Vichnevetsky, AICA, Rutgers University, 346–356, 1975.

⁴ Few textbooks deal with the subject more than a superficial “recipe” level. The terminology is not standardized. A typical example is Cook, Malkus and Plesha, who present stress hybrids following Pian’s original 1964 treatment and stop there. Even a more advanced monograph such as Oden and Reddy, cited in §3.6.2, covers hybrid functionals as an afterthought.

⁵ And sometimes, in the case of curved shell elements based on shell theory, impossible.

FIGURE 9.1. Slicing a body of volume V by an internal boundary S_i .

Indeed mixed methods do a good job for one-dimensional elements, as exemplified in Chapters 6 and 7. These improvements can be extended to 2D and 3D elements of particularly simple shapes, such as rectangles and cubes.

For 2D and 3D continuum elements of general shape, however, pure mixed methods run into implementation and numerical difficulties, which are too complex to describe here. To date they have not achieved the success of hybrid methods and there are reasons to argue that they never will.⁶

Note that the foregoing statement is qualified: it says “pure mixed functionals” — see the classification in (9.1). The classical HR and VHW functionals covered in the previous Chapters belong to this category. But if mixed and hybrid functionals are combined, in the sense that the former are used for the interior region, very powerful element formulation methods emerge. Therefore, learning mixed functionals is not a loss of time.

§9.3. Slicing a Potato

To understand the idea behind hybrid functionals, consider again a potato-shaped elastic body of volume V and surface S . Slice it by a smooth internal interface S_i , as depicted in Figure 9.1. This allows the consideration of certain field discontinuities. Those discontinuities may be of physical or computational nature, as discussed later.

This interface S_i , also called an interior boundary, divides V into two subdomains: V^+ and V^- so that $S_i : V^+ \cap V^-$. The outward normals to S_i that emanate from these subdomains are denoted by \mathbf{n}^+ and \mathbf{n}^- , respectively. Note that at corresponding locations they point in equal but opposite directions. The external boundary is relabeled S_x ; thus the complete boundary is $S : S_x \cup S_i$. For many derivations it is convenient to view V^+ and V^- as disconnected subvolumes with matching boundaries S_i^+ and S_i^- , as illustrated in Figure 9.1.

§9.3.1. Traversing the Interior Boundary

To visualize the following property of internal boundaries it is convenient to consider a two-dimensional domain as in Figure 9.2. This is broken up into four pieces or subdomains as illustrated

⁶ One of the barriers has been the so-called “limitation principle” discovered in the early 1960s: B. M. Fraeijs de Veubeke, Displacement and equilibrium models, in *Stress Analysis*, ed. by O. C. Zienkiewicz and G. Hollister, Wiley, London, 145–197, 1965; reprinted in *Int. J. Numer. Meth. Engrg.*, Vol. 52, 287–342, 2001.

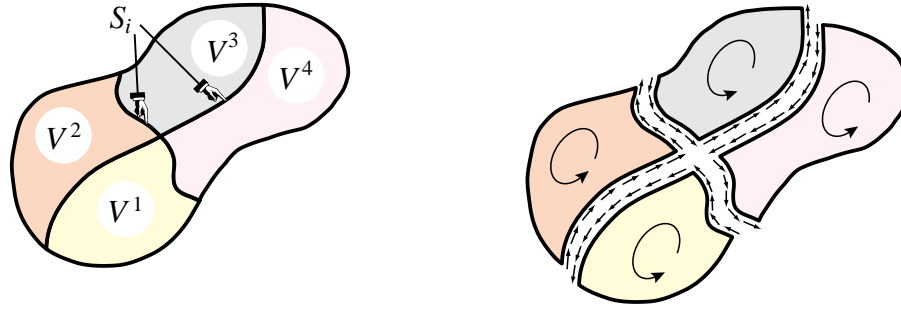


FIGURE 9.2. Slicing a two-dimensional body by an internal boundary divides it into 4 subdomains. Going around each subdomain in a counterclockwise path it is seen that S_i is traversed twice in opposite senses.

on the right of that figure. If these four subdomains are traversed counterclockwise to carry out an integration over S_i , note that each point of S_i is traversed twice, with normals pointing in opposite directions.

The same property is true in 3D because there are always two faces to an interface. However, the cancellation property is a bit more difficult to visualize by traversal.

§9.3.2. Volume and Surface Integrals

Going back to 3D, the volume and surface integrals that appear in conventional variational principles must be generalized as follows. An integral of function f over V becomes the sum of integrals over the separated volumes. If these are relabeled V^m , $m = 1, 2, \dots, M$ we get

$$\int_V f dV = \sum_{m=1}^M \int_{V^m} f dV. \quad (9.2)$$

The surface integral of a function g is split into contributions from the three boundaries

$$\int_S g dS = \int_{S_u} g dS + \int_{S_i} g dS + \int_{S_l} g dS. \quad (9.3)$$

As noted, the integral over S_i traverses twice over each face: $+$ and $-$, of the interface. Frequently the integrand g is of the flux form $g = \mathbf{f} \cdot \mathbf{n}$. Then if the components of \mathbf{f} are *continuous* on S_i , that integral cancels out because $\mathbf{n}^+ = -\mathbf{n}^-$ and consequently $\mathbf{f} \cdot (\mathbf{n}^+ + \mathbf{n}^-) dS \equiv 0$.

But if some components of the integrand are discontinuous, the interface integral will not necessarily cancel. This is the origin of hybrid principles.

§9.4. A Stress Hybrid Principle

A hybrid principle is obtained by adding two functionals:

$$\boxed{\text{Hybrid Principle} = \text{Interior Functional} + \text{Interface Potential}} \quad (9.4)$$

The *interior functional* is of the classical type studied in previous Chapters. The new ingredient is the *interface potential*, which comes from the contribution of the interface.

Rather than going for the most general form possible, in the following we construct the particular hybrid variational principle that gives rise to *equilibrium-stress hybrid elements*. Historically this was the first one derived by Pian (see footnotes in §9.2 and Exercise 9.3). It is still good for instructional purposes because it has a minimum number of ingredients. This principle is used to formulate a four-node plane stress quadrilateral element in the next chapter.

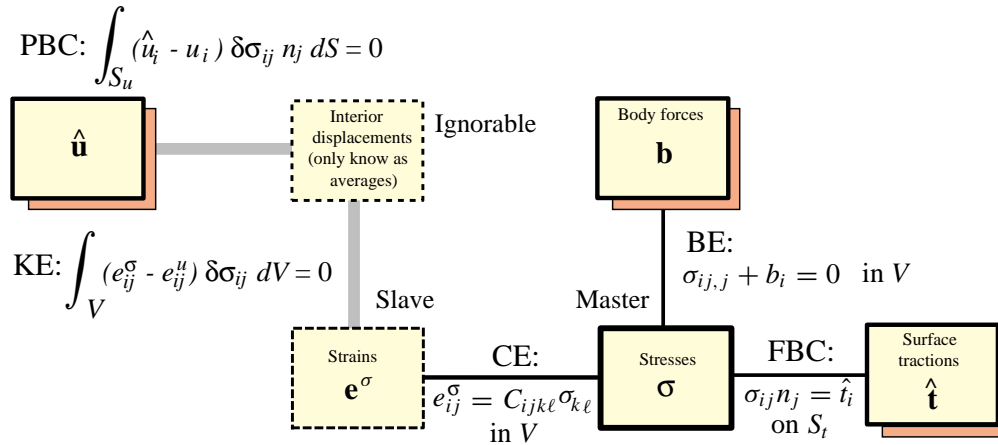


FIGURE 9.3. Schematics of Weak Form of TCPE principle of elasticity.

§9.4.1. The Variational Principle

The *interior functional* for this example is that of the total complementary potential energy (TCPE) principle of linear elastostatics:

$$\Pi_C[\sigma_{ij}] = -\frac{1}{2} \int_V \sigma_{ij} C_{ijkl} \sigma_{kl} dV + \int_{S_u} \hat{u}_i \sigma_{ij} n_j dS = -U_C + W_C. \quad (9.5)$$

Here U_C is the internal complementary energy in terms of stresses

$$U_C[\sigma_{ij}] = \frac{1}{2} \int_V \sigma_{ij} e_{ij}^\sigma dV = \frac{1}{2} \int_V \sigma_{ij} C_{ijkl} \sigma_{kl} dV, \quad (9.6)$$

which is stored in the body as elastic internal energy, and W_C is the work potential term of (9.5). This is a single-field functional with stresses as the only master field. The Weak Form for this principle is shown in Figure 9.3.

§9.4.2. Hybridization

To hybridize this principle, split V into M subvolumes V^m , $m = 1, 2, \dots, M$ by internal interfaces collected in S_i . (In the finite element applications, these subvolumes become the individual elements, to be relabeled with superscript e). Take a boundary displacement field d_i over S_i as additional master. This s-called *connector displacement field* must be unique on S_i . Its function is to link or connect subvolumes, functioning as a *frame*. The master stress field σ_{ij} is “glued” to the frame by

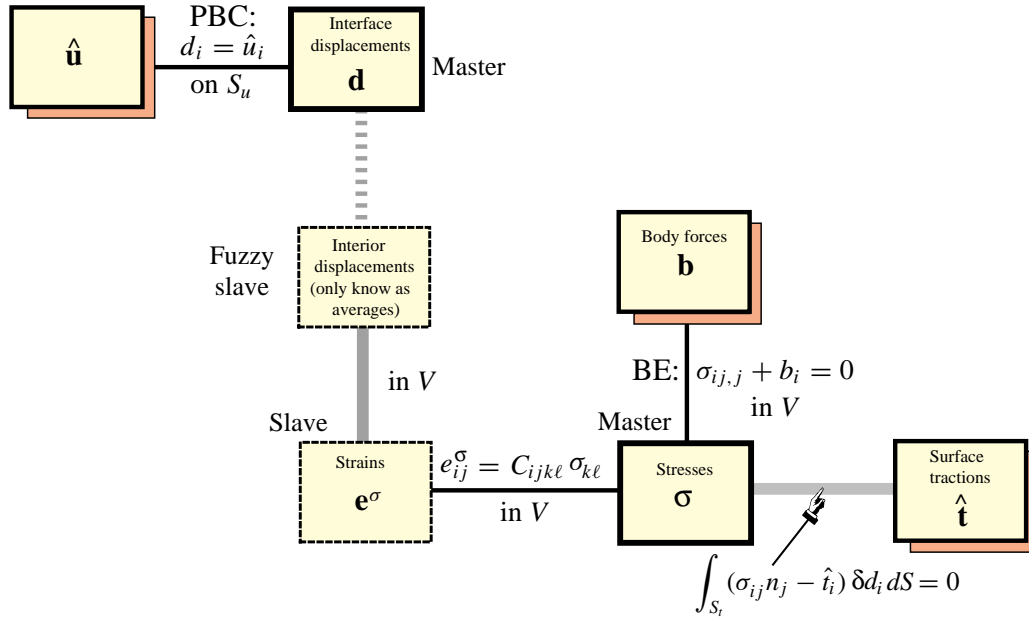


FIGURE 9.4. Schematics of Weak Form of the equilibrium-stress-hybrid principle. As a Tonti diagram this is still unsatisfactory; needs to be improved: suggestions welcome.

adding an integral π_d over S_i , called the *interface potential*, which measures the work lost or stored on S_i :

$$\Pi_C^d[\sigma_{ij}, d_i] = \Pi_C[\sigma_{ij}] + \pi_d[\sigma_{ij}, d_i] = \Pi_C[\sigma_{ij}] + \int_{S_i} d_i \sigma_{ij} n_j dS. \quad (9.7)$$

This is a *multifield* hybrid functional with two masters: the stresses σ_{ij} and the displacement field d_i . It is not a mixed functional because d_i is not an interior field, as it exists only over the interface S_i . The Weak Form for this principle is shown in the diagram of Figure 9.4.⁷ Comparing Figure 9.4 to Figure 9.3, it can be observed that link PBC has become strong whereas FBC is now weak. This is the result of the integral transformations worked out below.

Note that if the flux $t_j = \sigma_{ij} n_j$ is continuous across S_i , π_d vanishes, as explained after (9.3). This is characteristic of interface potentials: they vanish if there are no discontinuities.

§9.4.3. The Work Potential

The functional (9.7) can be decomposed into two functionally distinct parts

$$\Pi_C^d = -U_C + W_d \quad (9.8)$$

where U_C is the complementary energy (9.6), and W_d is the *work potential*

$$W_d = \int_{S_u} \hat{u}_i \sigma_{ij} n_j dS + \int_{S_i} d_i \sigma_{ij} n_j dS. \quad (9.9)$$

⁷ As noted in the legend, this diagram needs improvement. It does not show clearly the role of the interface potential. Suggestions welcome.

This term includes the work of the prescribed displacements on S_u as well as the energy stored or lost on the internal interface S_i . For finite element work it is necessary to transform the integral over S_i to one over $S = S_u \cup S_t \cup S_i$. Using the identity

$$\int_{S_i} d_i \sigma_{ij} n_j dS = \int_S d_i \sigma_{ij} n_j dS - \int_{S_u} d_i \sigma_{ij} n_j dS - \int_{S_t} d_i \sigma_{ij} n_j dS, \quad (9.10)$$

on the functional (9.9) we obtain

$$W_d = \int_S d_i \sigma_{ij} n_j dS - \int_{S_t} d_i \hat{t}_i dS \quad (9.11)$$

because the integral of $(\hat{u}_i - d_i) \sigma_{ij} n_j$ over S_u vanishes on account of the strong connection $d_i = \hat{u}_i$ on S_u . The last term comes from replacing $\sigma_{ij} n_j \rightarrow \hat{t}_i$ on S_t because of the original FBC strong connection (see Figure 9.3), which now becomes weak because d_i “interposes” between σ_{ij} and \hat{t}_i . Replacing into (9.8) we arrive at the final form

$$\Pi_C^d[\sigma_{ij}, d_i] = -U_C + W_d = -\frac{1}{2} \int_V \sigma_{ij} C_{ijkl} \sigma_{kl} dV + \int_S d_i \sigma_{ij} n_j dS - \int_{S_t} d_i \hat{t}_i dS. \quad (9.12)$$

The integral over S_u has disappeared while that over S_t , which has the same form as in the TPE functional except that u_i is replaced by d_i , comes into play. The specified displacement \hat{u}_i disappears into the strong connection $d_i = \hat{u}_i$ on S_u . Most important of all: the interface potential is taken over the whole boundary S , not just S_i .

Remark 9.1. Several finite element papers and textbooks do this transformation incorrectly and end up with erroneous boundary terms. The error is often inconsequential, however, as most element derivations take the “save S_u and S_t for last” route described later. But in nonlinear analysis errors can have serious consequences.

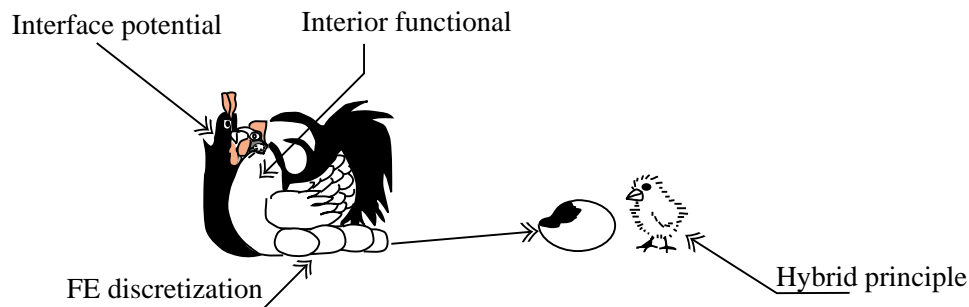


Figure 9.5. The chicken-and-egg story revisited: (a) An interior (non-hybrid) functional (the hen) and an interface potential (the rooster) beget a hybrid principle (the chick) in the sheltered framework of FEM.

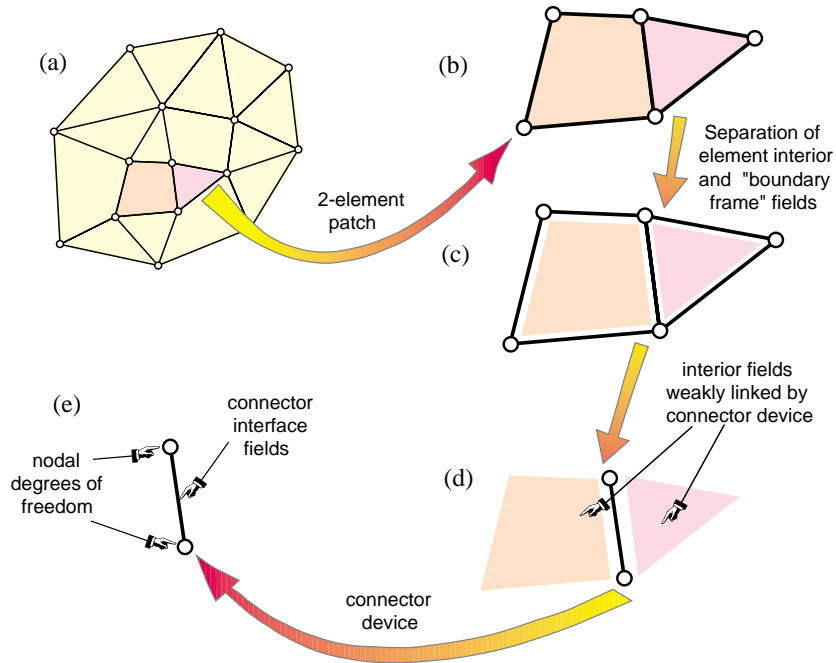


Figure 9.6. Conceptual steps in constructing hybrid finite elements. They are illustrated in 2D for visualization convenience.

§9.4.4. Hybrids or FEM: A Chicken and Egg Story

It has been said that finite elements are a byproduct of the advent of computers: no computers, no finite elements. A similar claim: “without finite elements there would be no hybrid variational principles” is too strong, because as noted in §9.2 these principles were also derived from a continuum mechanics standpoint. However, without finite elements they would have remained largely a mathematical curiosity. Figure 9.5 puts this observation into the context of the old chicken and egg story.

The conceptual steps in applying these principles to formulate individual finite elements are sketched in Figure 9.6. Note that the subdivision into elements comes *before* the principle is constructed; else there would be no S_i to integrate on. So the FE mesh is where the principle is realized and lives on.

§9.5. A 4-Node Plane Stress Hybrid Quadrilateral

We apply now Π_C^d to the construction of the 4-node plane-stress quadrilateral element shown in Figure 9.7. The element has constant thickness h and constant material properties characterized by the elastic compliance matrix $\mathbf{C} = \mathbf{E}^{-1}$ that relates strains to stresses: $\mathbf{e} = \mathbf{C}\boldsymbol{\sigma}$. For simplicity in the element construction we shall assume that the body force field \mathbf{b} vanishes.

This element has historical importance as being the first one to be derived (by Pian in 1964, reference given in §9.2). Although as noted later the element does not have good performance, it serves to illustrate the derivation steps.

§9.5.1. The Stress Field

The first ingredient is the internal stress field, which is a master. We assume that each component of the stress field $(\sigma_{xx}, \sigma_{yy}, \sigma_{xy})$ varies linearly in x and y :

$$\begin{aligned} \sigma_{xx} &= a_1 + a_4 x + a_5 y, \\ \sigma_{yy} &= a_2 + a_6 x + a_7 y, \\ \sigma_{xy} &= a_3 + a_8 x + a_9 y. \end{aligned} \quad (9.13)$$

The a_i are called the *stress-amplitude parameters*, or simply *stress parameters*, which function as generalized coordinates. If this field is to satisfy the homogeneous equilibrium equations for zero body forces:

$$\frac{\partial \sigma_{xx}}{\partial x} + \frac{\partial \sigma_{xy}}{\partial y} = 0, \quad \frac{\partial \sigma_{xy}}{\partial x} + \frac{\partial \sigma_{yy}}{\partial y} = 0, \quad (9.14)$$

then the stress coordinates cannot be independent but must verify the constraints

$$a_4 + a_9 = 0, \quad a_7 + a_8 = 0. \quad (9.15)$$

Substituting these into the expression for the shear stress in (9.13) gives $\sigma_{xy} = a_3 - a_7x - a_4y$. Consequently there are only *seven* independent stress parameters, which may be collected into a column vector \mathbf{a} . In matrix form:

$$\begin{bmatrix} \sigma_{xx} \\ \sigma_{yy} \\ \sigma_{xy} \end{bmatrix} = \begin{bmatrix} 1 & 0 & 0 & x & y & 0 & 0 \\ 0 & 1 & 0 & 0 & 0 & x & y \\ 0 & 0 & 1 & -y & 0 & 0 & -x \end{bmatrix} \begin{bmatrix} a_1 \\ a_2 \\ \vdots \\ a_7 \end{bmatrix}, \quad (9.16)$$

or

$$\boxed{\boldsymbol{\sigma} = \mathbf{S}\mathbf{a}} \quad (9.17)$$

Remark 9.2. Why (9.13)? Short answer: invariance plus rank sufficiency. In the foregoing derivation x and y are assumed to be the global axes. If the orientation of these axes changes by a rotation about z , the equilibrium stress expansion (9.16) varies in the sense that the stress parameter values change, but the resulting element (and the finite element solution for the assembled model) is *independent* of the orientation of the axes. This is a consequence of the expansion (9.13) being a *complete polynomial* in x and y . Finite elements that comply with this condition (namely, that the solution be independent of the choice of global axes) are called *observer invariant* or simply *invariant*. Stress assumptions that are complete polynomials lead to invariant elements. The simplest such choice is a constant stress assumption (a complete polynomial of order 0) but as noted in the following Remark, that choice leads to rank deficiency.

Remark 9.3. Had only three stress parameters been retained in the assumption (9.16), namely a_1 , a_2 and a_3 , which obviously satisfy the homogeneous equilibrium equations (9.14), the element stiffness $\mathbf{K}^{(e)}$ derived later would have rank three at most (because the flexibility matrix \mathbf{F} becomes 3×3). Since the target rank is $5 = 8 - 3$, the element stiffness matrix would be twice rank deficient and thus unacceptable.

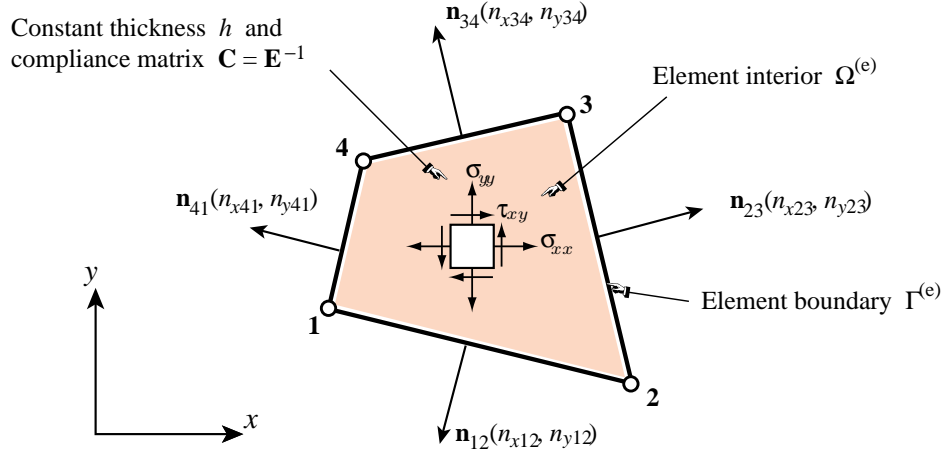


Figure 9.7. A 4-node stress-hybrid quadrilateral for plane stress analysis. For visualization convenience, the element interior is shown slightly separated from the element boundary.

§9.5.2. Boundary Displacements

The second master ingredient in the stress hybrid functional are the boundary displacements, d_i . To maintain interelement compatibility the displacement of side 1-2, say, should depend only on the displacements of nodes on that side. This requirement can be obviously satisfied by a linear interpolation of displacements along each side:

$$\begin{bmatrix} d_{x12} \\ d_{y12} \\ d_{x23} \\ \vdots \\ d_{y41} \end{bmatrix} = \frac{1}{2} \begin{bmatrix} 1 - \xi_{12} & 0 & 1 + \xi_{12} & 0 & 0 & 0 & 0 & 0 \\ 0 & 1 - \xi_{12} & 0 & 1 + \xi_{12} & 0 & 0 & 0 & 0 \\ 0 & 0 & 1 - \xi_{23} & 0 & 1 + \xi_{23} & 0 & 0 & 0 \\ \vdots & \vdots & \vdots & \vdots & \vdots & \vdots & \vdots & \vdots \\ 0 & 1 + \xi_{41} & 0 & 0 & 0 & 0 & 0 & 1 - \xi_{41} \end{bmatrix} \begin{bmatrix} u_{x1} \\ u_{y1} \\ u_{x2} \\ u_{y2} \\ \vdots \\ u_{y4} \end{bmatrix} \tag{9.18}$$

Here ξ_{ij} denotes an isoparametric side coordinate that goes from -1 at node i to $+1$ at node j . This equation may be written in compact matrix form as

$$\boxed{\mathbf{d} = \mathbf{P}\mathbf{u}} \tag{9.19}$$

where \mathbf{P} is an 8×8 matrix.

§9.5.3. Surface Traction

The slave surface tractions $t_i = \sigma_{ij}n_j$ associated with the assumed interior-stress field appear in the interface potential. For a 2D plane stress field referred to $\{x, y\}$ coordinates, the in-plane traction components are

$$t_x = \sigma_{xx}n_x + \sigma_{xy}n_y, \quad t_y = \sigma_{yx}n_x + \sigma_{yy}n_y. \tag{9.20}$$

Over each side the external normals have fixed direction; they will be identified by the notation of Figure 9.2. On side 1-2 the matrix form of (9.20) is

$$\begin{bmatrix} t_{x12} \\ t_{y12} \end{bmatrix} = \begin{bmatrix} n_{x12} & 0 & n_{y12} \\ 0 & n_{y12} & n_{x12} \end{bmatrix} \begin{bmatrix} \sigma_{xx} \\ \sigma_{yy} \\ \sigma_{xy} \end{bmatrix} = \mathbf{N}_{12} \boldsymbol{\sigma}_{12} = \mathbf{N}_{12} \mathbf{S}_{12} \mathbf{a} \quad (9.21)$$

where \mathbf{S}_{12} is \mathbf{S} evaluated on side 1-2. Repeating this construction for the other three sides we build the relation

$$\mathbf{t} = \mathbf{T} \mathbf{a} \quad (9.22)$$

where \mathbf{t} collects the 8 traction components, which are function of the coordinates through \mathbf{S} :

$$\mathbf{t} = [t_{x12} \quad t_{y12} \quad t_{x23} \quad t_{y23} \quad \cdots \quad t_{y41}]^T, \quad (9.23)$$

and \mathbf{T} is an 8×7 matrix obtained by appropriately “row stacking” the four 2×7 matrices $\mathbf{N}_{12} \mathbf{S}_{12}$, $\mathbf{N}_{23} \mathbf{S}_{23}$, $\mathbf{N}_{34} \mathbf{S}_{34}$ and $\mathbf{N}_{41} \mathbf{S}_{41}$.

§9.5.4. Specified Boundary Traction

As forces acting on the element we consider boundary tractions $\hat{\mathbf{t}}$ acting on the four sides, and specified per unit of side length and thickness. These are collected to form the 8-vector

$$\hat{\mathbf{t}} = [\hat{t}_{x12} \quad \hat{t}_{y12} \quad \hat{t}_{x23} \quad \hat{t}_{y23} \quad \cdots \quad \hat{t}_{y41}]^T. \quad (9.24)$$

§9.5.5. The Discrete Equations

Inserting (9.17), (9.19), (9.22) and (9.24) into the functional Π_C^d for an individual element we get

$$\Pi_C^d = -\frac{1}{2} \mathbf{a}^T \mathbf{F} \mathbf{a} + \mathbf{a}^T \mathbf{G} \mathbf{u} - \mathbf{f}^T \mathbf{u}, \quad (9.25)$$

in which the element identification superscript has been omitted from matrices and vectors for brevity. The matrices in (9.25) are given by

$$\mathbf{F} = \int_{\Omega^{(e)}} h \mathbf{S}^T \mathbf{E}^{-1} \mathbf{S} d\Omega, \quad \mathbf{G} = \int_{\Gamma^{(e)}} h \mathbf{T}^T \mathbf{P} d\Gamma, \quad \mathbf{f} = \int_{S^{(e)}} h \hat{\mathbf{t}} \mathbf{P} d\Gamma. \quad (9.26)$$

Matrix \mathbf{F} is often called a flexibility matrix, hence the identifying symbol.

Rendering Π_C^d (now an algebraic function) stationary with respect to the stress and displacement degrees of freedom we get

$$\frac{\partial \Pi_C^d}{\partial \mathbf{a}} = -\mathbf{F} \mathbf{a} + \mathbf{G} \mathbf{u} = \mathbf{0}, \quad \frac{\partial \Pi_C^d}{\partial \mathbf{u}} = \mathbf{G}^T \mathbf{a} - \mathbf{f} = \mathbf{0}. \quad (9.27)$$

The first equation is a discrete version of KE (the kinematic or compatibility relation), whereas the second one is a discrete form of BE, the balance or equilibrium equation.⁸

⁸ Recall that the KE and BE links are weak in this hybrid principle; cf. Figure 9.4.

Now if matrix \mathbf{F} is invertible we may solve for the \mathbf{a} vector at the element level from the first of (9.27) as $\mathbf{a} = \mathbf{F}^{-1}\mathbf{G}\mathbf{u}$, because the stress parameters are “disconnected” from element to element. Substituting into the second of (9.27) yields

$$\mathbf{G}^T \mathbf{F}^{-1} \mathbf{G} \mathbf{u} - \mathbf{f} = \mathbf{0}. \quad (9.28)$$

But these are formally the element stiffness equations, which on restoring the element superscript, become

$$\mathbf{K}^{(e)} \mathbf{u}^{(e)} = \mathbf{f}^{(e)}, \quad (9.29)$$

in which

$$\mathbf{K}^{(e)} = \mathbf{G}^T \mathbf{F}^{-1} \mathbf{G} \quad (9.30)$$

is the element stiffness matrix. The dimensions of \mathbf{G}^T , \mathbf{F} and \mathbf{G} are 8×7 , 7×7 and 7×8 , respectively. The expected rank of $\mathbf{K}^{(e)}$ is $5 = 8 - 3$, which is the dimension of $\mathbf{K}^{(e)}$ minus the number of independent rigid body modes. The rigid body modes are injected by the matrix \mathbf{G} .

Remark 9.4. \mathbf{F} is called a *flexibility matrix* in terms of the stress parameters \mathbf{a} , whereas \mathbf{G} is called the *connection matrix*, or *leverage matrix* in the literature. The transpose \mathbf{G}^T is called the *equilibrium matrix*.

Remark 9.5. The supermatrix form of (9.27) is

$$\begin{bmatrix} -\mathbf{F} & \mathbf{G} \\ \mathbf{G}^T & \mathbf{0} \end{bmatrix} \begin{bmatrix} \mathbf{a} \\ \mathbf{u} \end{bmatrix} = \begin{bmatrix} \mathbf{0} \\ \mathbf{f} \end{bmatrix}, \quad (9.31)$$

which displays the characteristic configuration for hybrid elements of this type. (Compare the discussion of “connector elements” in §6.4.) Static condensation of \mathbf{a} by forward Gauss elimination yields the stiffness equation (9.29).

§9.5.6. Is This Element Any Good?

Historically the foregoing element was the first stress hybrid model for plane stress analysis. Numerical experiments show that the element is better for bending-like behavior than the 4-node isoparametric bilinear quadrilateral developed in IFEM. However, the improvement is marginal and would not justify the far more complex construction. Why? The key reason is that the proper rank of the stiffness matrix is five = $8 - 3$. That would be the ideal number of *independent* stress parameters a_i , no more and no less. But instead we have used seven in (9.16).

How can the number of stress parameters be cut to 5? One solution, discovered (and re-discovered) by many authors, is to set $a_4 = a_7 = 0$ so that after renumbering the parameters the equilibrium stress field assumption effectively reduces to

$$\begin{aligned} \sigma_{xx} &= a_1 + a_4 y, \\ \sigma_{yy} &= a_2 + a_5 x, \\ \sigma_{xy} &= a_3. \end{aligned} \quad (9.32)$$

which in matrix form is

$$\begin{bmatrix} \sigma_{xx} \\ \sigma_{yy} \\ \sigma_{xy} \end{bmatrix} = \begin{bmatrix} 1 & 0 & 0 & y & 0 \\ 0 & 1 & 0 & 0 & x \\ 0 & 0 & 1 & 0 & 0 \end{bmatrix} \begin{bmatrix} a_1 \\ a_2 \\ a_3 \\ a_4 \\ a_5 \end{bmatrix}. \quad (9.33)$$

This assumption improves the element behavior while reducing formation cost. Unfortunately it has a significant drawback: the element is *no longer observer-invariant* with respect to the choice of axes x and y because (9.32) are not complete polynomials (cf. Remark 9.1). Aligning x and y with the global axes now would give *finite element solutions that depend on orientation*, which is obviously highly undesirable as well as scary to a naive user.

The usual solution to this dilemma: balanced stiffness versus invariance, is to chose (9.32) in a *local Cartesian system* (\bar{x}, \bar{y}) which is *attached* to the element in a “natural” way. For a rectangular geometry the obvious choice is to align (\bar{x}, \bar{y}) with the side directions. The resulting element is widely recognized to be the optimal one for this nodal DOF configuration.⁹ But for *arbitrary quadrilateral* geometries the choice of local system is far from obvious and has been the topic of substantial research.

Some authors have tried to recast the equilibrium equations (9.14) in isoparametric coordinates (ξ, η) , a process that automatically fulfills invariance but greatly complicates the stress assumption because such equations become quasilinear partial differential equations.

⁹ In fact the same quadrilateral element coalesces with those obtained from other high-performance element derivation methods, which is one of the characteristics of optimality.

Homework Exercises for Chapter 9

Hybrid Variational Principles of Elastostatics I

EXERCISE 9.1 [A:15] Present the derivation steps of the stress hybrid principle for a prismatic bar of constant cross section and modulus. Is the hybrid functional different from Hellinger-Reissner's?

EXERCISE 9.2 [A:20] Present the derivation steps of the stress hybrid principle for a prismatic plane Bernoulli-Euler beam of constant inertia and modulus. Is the hybrid functional different from Hellinger-Reissner's?

EXERCISE 9.3 [A:20=10+10] In a recent article, Pian¹⁰ reminisces on some events that led, through serendipity, to the formulation of the first hybrid elements in 1963.¹¹ He says that the initial investigation started from the Hellinger-Reissner principle for zero body forces ($b_i = 0$). Following is a variationally correct version of his arguments. In the notation of this course a "generalized HR" that extends HR with weak links to displacement BCs, reads

$$\Pi_{\text{HR}}^g[\sigma_{ij}, u_i] = -U^*[\sigma_{ij}] + \int_V \sigma_{ij} e_{ij}^u dV - \int_{S_t} \hat{t}_i u_i dS - \int_{S_u} \sigma_{ij} n_j (u_i - \hat{u}_i) dS, \quad (\text{E9.1})$$

where $U^*[\sigma_{ij}] = \frac{1}{2} \int_V \sigma_{ij} C_{ijkl} \sigma_{kl} dV$.

(a) Assume that σ_{ij} satisfies strongly the zero-body-force equilibrium equations $\sigma_{ij,j} = 0$. Transform (E9.1) via integration by parts using

$$\int_V \sigma_{ij} e_{ij}^u dV = - \int_V \overset{0}{\sigma_{ij,j}} u_i dV + \int_S \sigma_{ij} n_j u_i dS = \int_{S_t} \sigma_{ij} n_j u_i dS + \int_{S_u} \sigma_{ij} n_j u_i dS + \int_{S_i} \sigma_{ij} n_j u_i dS, \quad (\text{E9.2})$$

to get

$$\Pi_{\text{HR}}^g[\sigma_{ij}, u_i] = -U^* + \int_{S_u} \sigma_{ij} n_j \hat{u}_i dS - \int_{S_t} (\hat{t}_i - \sigma_{ij} n_j) u_i dS + \int_{S_i} \sigma_{ij} n_j u_i dS. \quad (\text{E9.3})$$

(Check this out.)

(b) Using the surface-integral identity (9.10) as appropriate, show that (E9.3) reduces to the stress hybrid functional (9.12) by identifying $d_i \equiv u_i$ on S and making $u_i = \hat{u}_i$ on S_u strong.

According to Pian that is roughly the way the stress hybrid principle eventually was linked to HR in the late 1960s.¹²

¹⁰ T. H. H. Pian, Some notes on the early history of hybrid stress finite element method, *Int. J. Numer. Meth. Engrg.*, **47**, 2000, 419-425.

¹¹ During a Fall Semester 1993 graduate course entitled Variational and Matrix Methods in Structural Mechanics, offered at MIT's Aero & Astro Department. According to Pian, the method grew out of assignments for the last class, which illustrated the use of the Hellinger-Reissner functional for the construction of element stiffness matrices. Eric Reissner was then a Professor at MIT and was of course influential in young Pian's research. Nobody else at the time had thought of using multifield functionals for FEM work, except for Len Herrmann at UC Davis.

¹² In the article cited above there are several variational errors: omission of the S_u term of (E8.1), no S_j and no transformation of the interface term to the whole surface S . The errors seem to compensate (two wrongs make a right). Pian's arguments are not easy to follow and are stated for a discrete functional, not a continuous one.

EXERCISE 9.4

[C:20] Form the 8×8 stiffness matrix \mathbf{K} of the hybrid 4-node, plane stress element defined by the stress assumptions (9.27). Restrict the geometry to a *rectangular* element of dimensions L along x and H along y . The material may be assumed isotropic, with elastic modulus E and Poisson's ratio ν . The thickness h is uniform.

Although computations may be done by hand (with enough patience it would take a couple of days) the use of a symbolic algebra system is highly recommended. Note: a *Mathematica* script is posted in Chapter 8 index to help.

EXERCISE 9.5

[A:20] Extend the stress hybrid principle (9.12) to include linear isotropic thermoelasticity. Assume that if the temperature T changes by $\Delta T = T - T_0$ from a reference value T_0 , the body expands isotropically with coefficient α . Hint: the indicial-form strain-stress equations become

$$e_{ij} = C_{ijkl}\sigma_{kl} + \alpha\Delta T\delta_{ij}, \quad (\text{E9.4})$$

where δ_{ij} is the Kronecker delta. The total complementary energy to be used in Π_C^d is $U^*[\sigma_{ij}] = \frac{1}{2} \int_V (\sigma_{ij}C_{ijkl}\sigma_{kl} + \alpha\Delta T\delta_{ij}\sigma_{ij}) dV$. Here $\delta_{ij}\sigma_{ij} = \sigma_{11} + \sigma_{22} + \sigma_{33} = \text{Trace}(\sigma_{ij}) = I_1$, the first invariant of the stress tensor, which is thrice the mean pressure.

EXERCISE 9.6

[A:20] Work out the inclusion of thermoelasticity effects, as outlined in the previous Exercise, into the formulation of the hybrid plane stress quadrilateral developed in §9.3. Show that an initial force vector \mathbf{f}_i has to be added to \mathbf{f} , and find its expression in terms of \mathbf{S} , \mathbf{G} , ΔT and α .